

Kinetics and Energetics in Nanolubrication

*René M. Overney*¹, *George Tyndall*² and *Jane Frommer*²

Lubrication, one of mankind's oldest engineering disciplines, in the 19th century gained from Reynolds' classical hydrodynamic description a theoretical base unmatched by most of the theories developed in Tribology to date. In the 20th century, however, increasing demands on lubricants shifted the attention from bulk film to ultrathin film lubrication. Finite size limitations imposed constraints on the lubrication process that were not considered in bulk phenomenological treatments introduced by Reynolds. At this point, as is common in many engineering applications, empiricism took over. Functional relationships derived from the classical theories were tweaked to accommodate the new situation of reduced scales by introducing "effective" or "apparent" properties.

With the inception of nanorheological tools of complementary nature in the later decades of the 20th century (e.g., the surface forces apparatus and scanning force microscopy) tribology entered the realm of nanoscience. Through an increasing confidence in experimental findings on the nanoscale, kinetic and energetic theories incorporated interfacial and molecular constraints.

The very fundamentals have been challenged in recent years. Researchers have realized that bulk perceptions, such as "solid" and "liquid", are defied on the nanoscale. The reduction in dimensionality of the nanoscale imposes constraints that bring into question the use of classical statistical mechanics of decoupled events. The diffusive description of lubrication is failing in a system that is thermodynamically not well-equilibrated.

The challenge any nanotechnological endeavor encounters is the development of a theoretical framework based on an appropriate statistics. In tribology this is met with spectral descriptions of the dynamic sliding process. Statistical kernels are being developed for probability density functions to explain anomalous transport processes that involve long-range spatial or temporal correlations. With such theoretical developments founded in nanorheological experiments, a more realistic foundation will be laid to describe the behavior of lubricants in the confined geometries of the nanometer length scale.

1. Introduction	2
2. Background: From Bulk to Molecular Lubrication	3
3. Thermal Activation Model of Lubricated Friction	5
4. Functional Behavior of Lubricated Friction	7
5. Thermodynamical Models Based on Small and Non- Conforming Contacts	8
6. Limitation of the Gaussian Statistics – The Fractal Space	10
7. Fractal Mobility in Reactive Lubrication	11
8. Metastable Lubricant Systems in Large Conforming Contacts	13
9. Conclusion	14
References	14

¹ University of Washington, Department of Chemical Engineering, Seattle, WA 98195-1750,
roverney@u.washington.edu

² IBM Almaden Research Center, San Jose, CA 95120

What is inaccessible today may become accessible tomorrow as has happened by the invention of the microscope ... Coherent assumptions on what is still invisible may increase our understanding of the visible ... Strong reasons have come to support a growing probability, and it can finally be said the certainty, in favor of the hypothesis of the atomists.

Jean Baptiste Perrin – Nobel Lecture,
December 11, 1926

1. Introduction

Since technology is driving lubricant films to molecular thickness, kinetic friction and its dependence on the sliding parameters - especially the sliding velocity - have become of great interest. The complexity of the frictional resistance in lubricated sliding is illustrated in Figure 1 with a *Stribeck Curve*. Various regimes of lubrication can be identified in the Stribeck curve. They express to what degree the hydrodynamic pressure is involved in the lubrication process. In the ultra-low speed regime, called the *boundary lubrication regime*, no hydrodynamic pressure is built up in the lubricant. Consequently the load is carried by contact asperities coated with adsorbed lubricant molecules. If the speed is raised, a hydrodynamic pressure builds that leads to a *mixed lubrication* in which the load is carried by both asperities and hydrodynamic pressure. At even higher speeds, elastic contributions of the solid surfaces have to be considered paired with hydrodynamic pressure effects (elastohydrodynamic lubrication), until only *hydrodynamic lubrication* matters. Hence, the Stribeck curve combines various aspects of lubrication. The curve cannot be discussed without considering the lubricant thickness and the different models of asperity contact sliding.

In one of the first comprehensive physical models of "dry" friction, Bowden and Tabor introduced a plastic asperity model, in which the material's yield stress and adhesive properties play an important role (Bowden et al. (1951)). Considering this model, which depends on surface energies and mechanical yield properties paired with all the properties that come along with a surface adsorbent lubricant, one can hardly grasp the difficulty level involved in describing the frictional kinetics in lubrication.

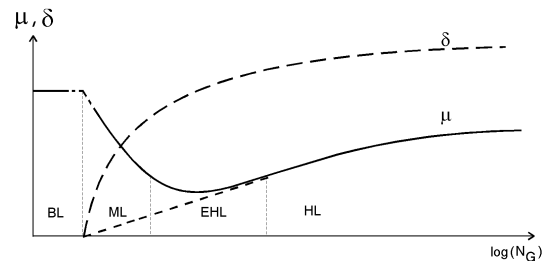


Figure 1. Stribeck Curve (schematic) relates the fluid lubricant thickness, δ , and the friction coefficient μ to the Gumbel Number $N_G = \eta \omega P^{-1}$; i.e., the product of the liquid bulk viscosity, η , the sliding speed (or more precisely the shaft frequency), ω , and the inverse of the normal pressure, P . BL: Boundary Lubrication, ML: Mixed Lubrication, EHL: Elastohydrodynamic Lubrication, HL: Hydrodynamic Lubrication.

Past and current engineering challenges in lubrication have been met with great and complex empiricism. The theoretical modeling of lubrication junctions generally involved only bulk property considerations with inadequately known adsorption mechanisms. The complexity of today's lubricants, most of them, such as motor oil, a product of empirical design over many years, increased exponentially, making it very difficult to meet future challenges. The problem of empiricism is that conventional laws and perceptions are unchallenged. *Effective* quantities are invented (e.g., effective viscosity), exponential fitting parameters are introduced (e.g., Kohlrausch relaxation parameter), and terminologies such as *solid* and *liquid* are taken as granted. Progress based on empiricism is only incremental and rarely revolutionary.

One of the reasons for empiricism is a lack of access to a system with fewer and better controlled parameters. In lubrication sliding that challenge has been addressed over the last two decades with the inception of the surface forces apparatus (SFA) by Tabor et al. (1969) and scanning force microscopy (SFM) by Binnig et

al. (1986). These two instrumental methods allow lubrication studies where roughness effects can be neglected, surface energies controlled, and wear from wearless friction distinguished. Lubricant properties can be studied at nearly mathematically described boundaries, atomistic friction events can be recorded, and fundamental models that have been considered to be mere Gedanken Experiments, such as the *Tomlinson model of friction*, can be verified. In the wake of these nanoscopic tools, exciting new theoretical lubrication and friction models have appeared.

This chapter considers these recent experimental and theoretical developments with a particular focus on sliding speed and real or apparent changes in the lubricant material properties. We will discuss kinetics and energetics in the "simplified" world of nanolubrication, in which our conventional perception is challenged. After a brief review of some of the classical lubrication concepts (hydrodynamic lubrication and boundary lubrication), we will turn our attention to a thermal activation model of friction, functional behavior of lubricated friction with velocity, and models based on small non-conforming contacts. We will critically discuss the limitation of the underlying Gaussian statistics, introduce fractal dynamics in lubrication, and will end our discussion with metastable lubricant systems.

2. Background: From Bulk to Molecular Lubrication

2.1 Hydrodynamic Lubrication and Relaxation

In the classical theories of tribology by da Vinci, Amontons, and Coulomb, not much attention was given to the dependence of kinetic friction on the sliding velocity. This clearly changed in the 19th century during the first industrial revolution, at which time lubricants became increasingly important, for instance, in ball and journal bearings. It was Petrov (1883), Tower (1883), and Reynolds (1886) who established that the liquid viscous shear properties determine the frictional kinetics. Reynolds (1886) combined the pressure-gradient determined *Poiseuille flow* with the bearing surface induced *Couette flow* assuming, based

on Petrov's law (Petrov (1883)), a no-slip condition at the interface between lubricant and solid. This led to the widely used linear relationship between friction and velocity. Reynolds' hydrodynamic theory of lubrication can be applied to steady state sliding at constant relative velocity and to transient decay sliding (sliding is stopped from an initial velocity v and a corresponding shear stress τ_o), which leads to the classical Debye exponential relaxation behavior, i.e.;

$$\tau = \tau_o \exp\left(\frac{-D}{A\eta}t\right); \quad \tau_o \propto \frac{v\eta}{D}. \quad (1)$$

D is the lubricant thickness, A the area of the slider, and η the viscosity of the fluid. We will later see that this classical exponential relaxation behavior, obtained in a thermodynamically well-mixed three dimensional medium, is distorted when the liquid film thickness is reduced to molecular dimensions.

2.2 Boundary Lubrication

Reynolds hydrodynamic description of lubrication was found to work well for thick lubricant films but to break down for thinner films. One manifestation is that for films on the order of ten molecular diameters, the stress in the film does not allow the tension to return to zero. It was also found that the motion in the steady state sliding regime was disrupted, exhibiting a stick-slip-like slider motion (Israelachvili et al. (1990)). Consequently, this non-Newtonian behavior was treated with a modified viscosity parameter (effective viscosity), which was composed of the pressure, temperature and rate of shear.

The term *Boundary Lubrication* is used to describe a lubricant that is reduced in thickness to molecular dimension and effectively reduces friction between two opposing solid surfaces. Hardy et al. (1922) recognized that molecular properties, such as molecular weight and molecular arrangement, are governing the frictional force. This confined concept of lubrication, often visualized by two highly ordered opposing films with shear taking place somewhere in between the two layers, contains many of the rate dependent manifestations of frictional sliding; e.g., stick-slip, ultra-low friction, transitions from high to low friction,

phase transitions, dissipation due to dislocations (e.g., gauche and cis-transformations), and memory effects.

Boundary lubrication was found to be in many respects unique (Dorinson et al. (1985)). In macroscopic experiments, which involved rough surfaces, friction-velocity plots resembled logarithmic functions at moderate speeds. No static friction force peaks were observed in boundary lubricants close to zero speed. On the contrary, retractive slips could be observed upon halting, constituting a static friction coefficient exceeded by the dynamic friction coefficient (Dorinson et al. (1985)). These unique manifestations of boundary lubrication were discussed in terms of a lubricated asperity-junction mechanism, which associated "an increase in the coefficient of friction with a decrease in the adsorptive coverage of the rubbing surfaces by the lubricant substance" (Dorinson et al. (1985)). It was argued that in the course of the sliding process of a macroscopic slider, more adsorbed lubricant is expected to exist within the interfacial area than outside. This would lead upon halting to a relaxation process of the elastic restraints on the slider, causing the slider to a retractively slip

2.3 Stick Slip and Collective Phenomena

Based on numerous friction experiments at the initiation of sliding with rough macroscopic contact, it was argued that the distinction between static and kinetic friction is not categorical but rather a manifestation of the apparatus (Dorinson et al. (1985)). This was a widely held opinion prior to Briscoe et al. (1982)'s molecularly smooth monolayer SFA experiments of aliphatic carboxylic acids and their soaps. Briscoe found that the character of sliding motion (continuous vs. discontinuous), depends not only on the apparatus but also on the properties (chemistry) of the monolayer. As in the rough boundary layer experiments discussed above, Briscoe's molecularly smooth monolayer experiments exhibited logarithmic-like friction-velocity behaviors

It was Israelachvili et al. (1990) who, based on SFA experiments and computer simulations, provided a molecular picture of the stick-slip behavior caused by the lubricant material. The major achievement of this work was to draw our

attention to the molecular structure of the lubricant, which is often different from the bulk, and unstable during the sliding motion. It was recognized that bulk rheology failed to describe the lubrication process. Finally addressed in the Israelachvili study were in-plane structuring of simple liquids caused by compression forces and "freezing-melting" transitions due to shear.

The simple concept of a freezing-melting transition is based on a common perception of the two distinctive parts of a stick-slip occurrence: the solid (Hookian)-like sticking part and the liquid (Newtonian)-like slipping part. But a deformation of a solid can be both, coordinated or uncoordinated, and thus can exhibit both solid-like and liquid-like behavior. For instance, most of the plastic yielding processes are uncoordinated. On the other hand, slipping within a solid, along a crystal plane in a thermally activated strain-release process for instance, is a highly coordinated molecular process (Blunier et al. (1992)).

Similar arguments can be made for a liquid. For example, stick-slip behaviors were observed in more complex fluidic systems by Reiter et al. (1994), who compared a molecularly "wet" lubricant film with a "dry" self-assembled monolayer lubricant. They concluded that sliding in liquid films is the result of slippage along an interface. In other words, the degree of molecular cooperation determined the frictional resistance.

The concept of local-*versus*-cooperative yield to shear is briefly illustrated here with a frictional-load study of a molecularly entangled polymer melt obtained in a SFM study of Buenviaje et al. (1999). Each of the curves presented in Figure 2(a) represents a polymer film of polyethylene co-propylene of distinctly different degree of entanglement. Films of thickness above 230 nm exhibit the strongest entanglement strength. Films of 20 nm thickness or thinner are fully disentangled. The reason for the film thickness-dependent entanglement strength is given by the substrate distance-dependent shear strength during the spin coating process of the thin films. For entangled films SFM friction studies exhibit a critical applied load (identified by P_c and the thickness t) that separates two friction regimes: One identified by a high friction coefficient and the other by a low

friction coefficient. At loads below P_t the friction coefficients are high, indicating plastic yielding during sliding. In these plastic regimes of sliding, molecular cooperation is low, leading to high local shear stresses compensated by local yielding of the material. Above the critical load, the friction coefficient drops, independent of the film thickness, to a low value of 3.0, corresponding to the value obtained from the fully disentangled film. Note that the polymer molecules in the 20-nm-thick film experience high substrate tangential stresses during the spin coating process.

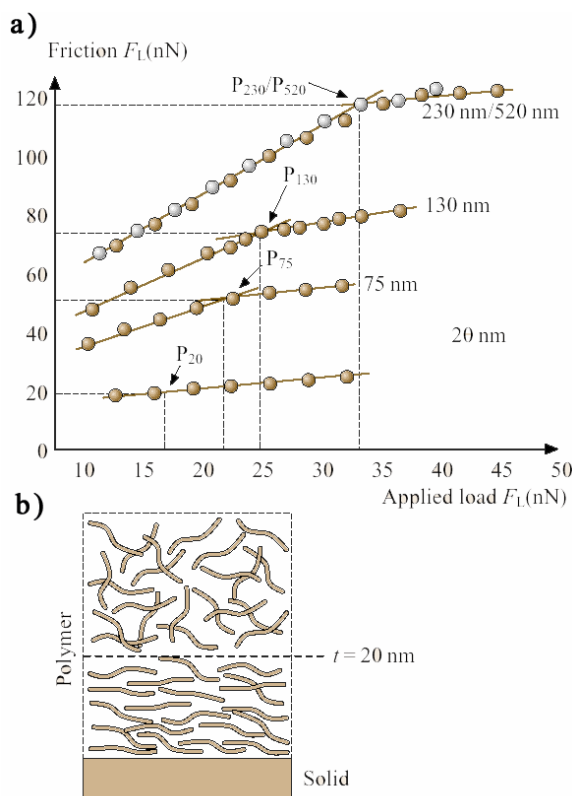


Figure 2. (a) SFM friction measurements at a speed 1 $\mu\text{m/s}$: Cooperative molecular response of polyethylene copolymer to frictional shear forces as a function of the applied load. P_t (t corresponds to the thickness of the polymer film) represents the critical activation load at which collective sliding is energetically more favorable than local plastic yielding. Adapted from Buenviaje et al. (1999). (b) Sketch of the degree of disentanglement in the vicinity to the solid substrate surface.

Hence the disentangled polymer molecules can be considered to be aligned preferentially along the substrate surface as sketched in Fig. 2(b). This leads to a decrease of the structural entropy

the closer the material is to the solid substrate surface. Considering the matching friction coefficient of 0.3 above P_t for thicker films, we can assume that any entangled film above a critical load exhibits a similar molecular collective response toward shear as the 20 nm film during spin coating. The critical load and its related pressure represent a barrier that has to be overcome before a collective phenomenon is activated.

3. Thermal Activation Model of Lubricated Friction

With the discussion of shear in entangled polymer systems we have introduced structural entropy as one of the key players that affect frictional resistance in lubricants. We found that the structural entropy was affected by the load of the slider, which introduces an activation barrier in the form of a critical pressure. The terminology used here resembles the one of the Eyring theory of molecular liquid transport (Glasstone et al. (1941)).

Eyring discussed a pure liquid at rest in terms of a thermal activation model. The individual liquid molecules experience a "cage-like" barrier that hinders molecular free motion, because of the close packing in liquids. To escape from the cage an activation barrier needs to be surmounted. In Eyring's model, two processes are considered in order to overcome the potential barrier: (i) shear stresses and (ii) thermal fluctuations. The potential barrier in the thermal activation model is depicted in Figure 3 indicating the barrier modification by the applied pressure force P , and shear stress τ .

Briscoe et al. (1982) picked up on this idea to interpret the frictional behavior observed on molecularly smooth monolayer systems. Starting from the overall barrier height $E = Q + P\Omega - \tau\phi$ that is repeatedly overcome during a discontinuous sliding motion, using a Boltzmann distribution to determine the average time for single molecular barrier-hopping, and assuming a regular series of barriers and a high stress limit ($\tau\phi/kT > 1$), the following shear strength versus velocity v relationship was derived (Briscoe et al. (1982)):

$$\tau = \frac{k_B T}{\phi} \ln\left(\frac{v}{v_0}\right) + \frac{1}{\phi} (Q + P\Omega). \quad (2)$$

The barrier height, E , is composed of the process activation energy Q , the compression energy $P\Omega$, where P is the pressure acting on the volume of the junction Ω , and the shear energy $\tau\phi$, where τ is the shear strength acting on the stress activation volume ϕ . T represents the absolute temperature. The stress activation volume ϕ can be conceived as a process coherence volume and interpreted as the size of the moving segment in the unit shear process, whether it is a part of a molecule or a dislocation line. The most critical parameter in equation (2), v_o , is a characteristic velocity related to the frequency of the process and to a jump distance (discussed further below).

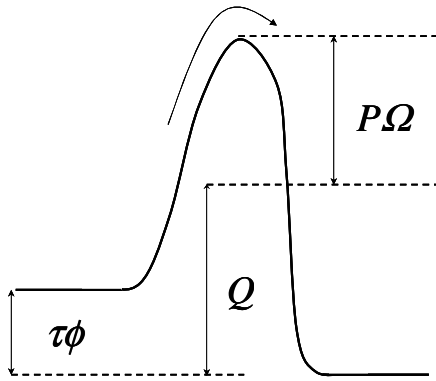


Figure 3. Potential barrier in a lubricant based on Eyring's thermodynamic "cage-model". The normal pressure P and the shear stress τ are modifying the barrier height Q . Modified from Briscoe et al. (1982).

From equation (2) the following iso-relationships can be directly deduced (Briscoe et al. (1982)):

$$\tau = \tau_o + \alpha P; \quad \tau_o = \frac{1}{\phi} \left(k_B T \ln \left(\frac{v}{v_o} \right) + Q \right); \quad \alpha = \frac{\Omega}{\phi};$$

at constant v , T (3a)

$$\tau = \tau_1 - \beta T; \quad \tau_1 = \frac{1}{\phi} (Q + P\Omega); \quad \beta = -\frac{k}{\phi} \ln \left(\frac{v}{v_o} \right);$$

at constant P , v (3b)

$$\tau = \tau_2 + \theta \ln v; \quad \tau_2 = \frac{1}{\phi} (Q + P\Omega - kT \ln v_o); \quad \theta = \frac{kt}{\phi}$$

at constant P , T . (3c)

Thus Eyring's model predicts a linear relationship of friction (the product of the shear strength and the active process area) in pressure

and temperature and a logarithmic relationship in velocity.

Eyring's model has been verified in lubrication experiments of solid (soap-like) lubricants by Briscoe and liquid lubricants by He et al. (2002) within three logarithmic decades of velocities. While Briscoe et al. (1982) employed a SFA that confines and pressurizes the film over several square microns, He et al. used a SFM system in which the contact is on the order of the lubricant molecular dimension.

He et al. determined the degree of interfacial structuring and its effect on lubrication of n-hexadecane and octamethylcyclotetra-siloxane (OMCTS). For spherically shaped OMCTS molecules, only an interfacial "monolayer" was found; in contrast, a 2-nm-thick entropically cooled layer was detected for n-hexadecane in the boundary regime to an ultra-smooth silicon wafer. SFM measurements of the two lubricants (with similar chemical affinity to silicon) identified the molecular shape of n-hexadecane responsible for augmented interfacial structuring. Consequently, interfacial liquid structuring was found to reduce lubricated friction, Fig. 4. Again as reasoned above, these results can be discussed in terms of a collective phenomenon, i.e., in terms of increased molecular coordination in n-hexadecane versus OMCTS.

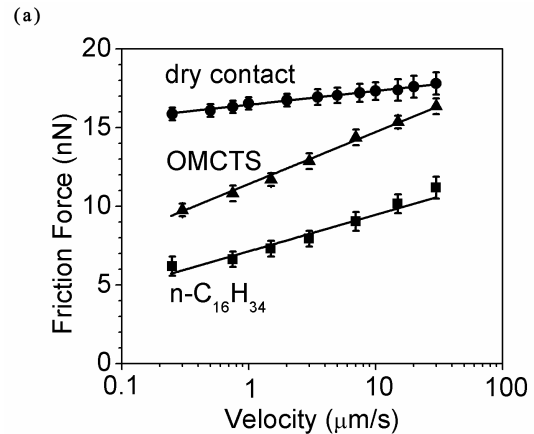


Figure 4 (a): Logarithmic $F_F(v)$ -plots. $F_F(v) = F_o + \alpha \ln(v[\mu\text{m/s}])$: • "dry" contact (18% relative humidity) with $F_o=16.4$ nN and $\alpha=0.91$ nN, ▲ OMCTS lubricated with $F_o=11.3$ nN and $\alpha=3.4$ nN, and ■ n-hexadecane ($n\text{-C}_{16}\text{H}_{34}$) lubricated with $F_o=7.1$ nN and $\alpha=2.5$ nN. The measurements were obtained with rectangular SFM cantilevers (0.4-0.8 N/m) at 100 nN load and 21 °C, both feedback-controlled.

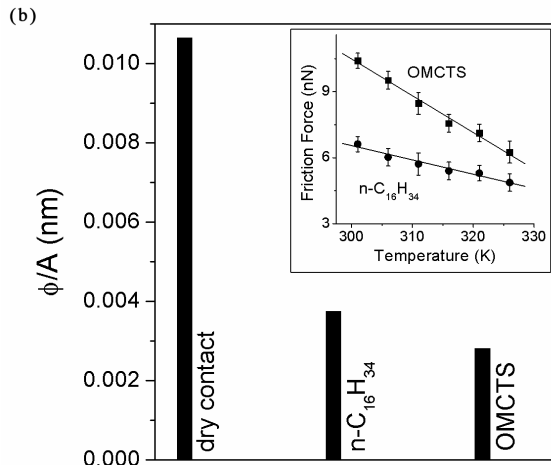


Figure 4 (b): Stress activation length, ϕ/A . (A area of contact) for OMCTS, n -hexadecane and dry contact. The inset provides a linear relationship between friction and temperature at a velocity of $1 \mu\text{m/s}$ and a normal load of 100 nN . Adapted from He et al. (2002).

4. Functional Behavior of Lubricated Friction

Friction-rate experiments are well suited to evaluate the rheological nature of interfacial liquids. In classical theories, such as the Reynolds' hydrodynamic theory discussed above, drag forces in lubricated sliding over thick liquid films were found to depend linearly on the rate of sliding and on the viscosity of the bulk fluid. In high-pressure lubrication, described by the elastohydrodynamic lubrication theory (Johnson (1987; Meyer et al. (1998)), it was found that the linear relationship between friction and velocity can be retained by adjusting the (apparent) viscosity by introducing an *apparent viscosity term*. Qualitatively, the same linear relationship has been observed for highly confined simple liquids between ultrasmooth mica surfaces such as alkanes (Christenson et al. (1987)). Note that the lubricated contact area in SFA experiments is on the micron-scale. It significantly exceeds the size of the confined molecules. For small and unbranched molecules, such as simple alkanes, it is possible that the confined material undergoes a pressure-induced phase reconstruction, which leads to material properties that deviate significantly from the bulk. Larger and more complex (branched) molecules are less likely to exhibit pressure-

induced phase reconstruction due to internal constraints and poor mixing within the contact area. This was shown by Drummond et al. (2000) in SFA shear experiments. They found that the linear friction-velocity dependence does not apply for branched hydrocarbon lubricants. Also Drummond discussed "molecular lubrication" in terms of a logarithmic friction-velocity relationship, which is in accordance with the above-discussed thermal activation model, the solid lubricant SFA study by Briscoe et al. (1982), and the liquid lubricant SFM study by He et al. (2002).

Common to the three studies by Briscoe, He, and Drummond is that they operate on a single material phase that is disrupted or relaxed over a very specific lateral length scale. In the Eyring model, the length scale is deduced by assuming a regular series of barriers, separated by a *virtual jump distance*. The distance is embedded in v_0 , the characteristic velocity, which is the product of the jump distance and the frequency of the process. Briscoe et al. (1982) used the lattice constant of the highly oriented monolayers as the virtual jump distance. It was assumed that the process frequency was related to the vibrational frequency of the molecules (10^{11} s^{-1}), neglecting sliding velocity, temperature, and pressure effects. He et al. (2002) assumed a jump distance of 0.2 nm and considered frequencies between a perfectly structured alkane layer (10^{11} Hz) and the bulk fluid ($10^{13} - 10^{15} \text{ Hz}$, estimated from infrared absorption data for typical covalent bonds). With these assumptions He determined total "jump-energies" of $4\text{-}8 \times 10^{-20} \text{ J}$. Briscoe and He pointed out that a friction-velocity study alone provides only a qualitative measure of the microscopic origin of friction. Additional measurements have to be conducted that quantitatively address jump distances and frequencies.

The issue of the jump distance has been addressed by Overney et al. (1994) in a SFM study on a highly ordered lubricant model system. This study avoided two levels of difficulties Briscoe et al. (1982) and He et al. (2002) encountered: (a) large contact areas of SFA studies, and (b) complex rheology with unknown structure parameters as in liquid lubricant studies. It involved contact dimensions

on the order of 1 nm^2 , and the crystalline form a bilayer model-lipid-lubricant with in-plane lattice spacings of 0.6 and 1.1 nm. The study mainly focused on the effect of the depth of the corrugation potential (barrier height) on the static and dynamic friction force. This is illustrated in Figure 5 in the form of stick-slip amplitude plotted as a function of the drag direction (i.e., sliding with respect to the anisotropic row-like film structure).

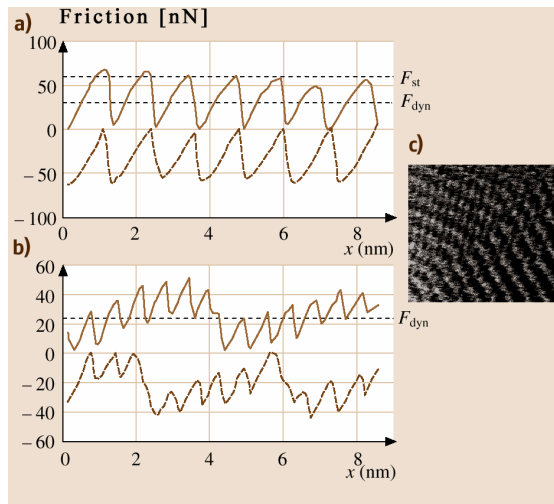


Figure 5. SFM molecular stick-slip measurements of a bilayer lipid system (5-(4'-N,N-dihexadecylamino)benzylidene barbituric acid). (a) and (b) are adapted from Overney et al. (1994a) and (c) from Overney et al. (1994b). (a) High amplitude frictional stick-slip behavior is observed for scans perpendicular to molecular rows as imaged in 5(c). F_{st} , static friction, is assigned to the maximum force occurrence. The average value corresponds to the dynamic friction value, F_{dyn} , determined on largescale micrometer scans. (b) A 30 degrees out of row direction scan leads to decreased frictional stick-slip behavior due to smaller molecular corrugations. (c) $12 \times 12 \text{ nm}^2$ SFM lateral force image of a highly structured lipid bilayer. Two crystalline domains with a boundary are imaged. The anisotropic row-like structure is responsible for directional dependent friction forces. The molecular corrugation between the rows is larger than the molecular corrugation in between a single row.

Relevant to our discussion about jump distance in lubrication events is Overney's discussion about the sliding speed and its effect on the slip distance. They demonstrated that within sliding speeds of 36 nm/s to 100 nm/s, the jump distance corresponded to the lattice spacing. At higher velocities, however, they could observe jumps over multiples of lattice

distances and found the jump length distribution to become increasingly stochastic at higher velocities. They proposed molecular (or atomistic) friction as a white-noise driven system, which obeys a Gaussian fluctuation-dissipation relation. Hence, based on this finding one should consider discussing kinetic friction in terms of a statistical fluctuation model and understand the jump distance as a statistical quantity.

5. Thermodynamical Models Based on Small and Nonconforming Contacts

The SFM approach simulates a single asperity contact with a very high compliance, provided by a microfabricated and etched ultra-sharp tip and a typically soft cantilever spring. From a realistic, tribological perspective, the SFM approach is targeted toward the study of the intrinsic lubricant properties of a thin film in close vicinity to the solid substrate. The small contact area on the order of the lubricant's molecular dimension allows discussing SFM results in terms of a thermodynamic equilibrium. The area is insufficient in reorganizing the lubricant molecules coherently, to cause an apparent material phase-transition, or to generate a metastable situation as observed in SFA experiments (see below). SFM is therefore not appropriate to reflect on tribological issues involving large area confinement effects.

In our prior molecular discussion of friction above, we introduced for solid and liquid lubrication a thermal activation model, the *Eyring model*, which employed a regular series of potential barriers. Note that the concept applies for a solid lubricant of an inherent, highly ordered structure (e.g., Briscoe et al. (1982)), but also for a liquid system in which the series of potentials is built up and overcome in the course of the shear process (e.g., He et al. (2002)).

Gnecco et al. (2000) showed in a ultrahigh vacuum study on sodium chloride that the concept of the Eyring model also applies for dry SFM friction studies. Thus a molecular theory of lubricated friction involving a molecular contact could be derived from a very simplistic model of an apparent sinusoidal-corrugated surface over which a cantilever tip is pulled. In a first attempt

one could assume that the corresponding wave length of the shear process corresponds to the apparent lattice spacing of the corrugated surface. With such a simple attempt it is, however, assumed that there is no noise, such as thermal noise, existing in the system, and thus, the driven tip leaves the total potential well when the barrier vanishes at the instability point. In the presence of noise, the transition to sliding can be expected to occur before the top of the barrier is reached. Such barrier-hopping fluctuations have been theoretically discussed by Sang et al. (2001) and Dudko et al. (2002).

The relationship between thermal fluctuations and velocity must be handled thoughtfully. Sang et al. (2001) pointed out that in previous considerations of thermal fluctuations by Heslot et al. (1994), the fluctuations were proportionally related to the velocity, which led to a friction force that is logarithmically dependent on the velocity. In Heslot's *linear creep model*, the barrier height is proportional to the frictional force. Sang argued that if one considered an absorbing boundary condition (i.e., an elastic deformation of the overall potential which is accomplished by shifting the x-axis) the barrier height becomes proportional to a 3/2-power law in the friction force. Sang's extended linear creep model resembles a *ramped creep model*, and leads analytically to a logarithmic distorted dynamic friction-versus-velocity relationship; i.e.,

$$F = F_c - \Delta F \left| \ln v^* \right|^{2/3}. \quad (4)$$

In equation (4) v^* represents a dimensionless velocity, $\Delta F \propto T^{2/3}$, and F_c is an experimentally determined constant (by plotting F versus $T^{2/3}$ for a fixed ratio $T/v = 1$ K/(nm/sec)) that contains the critical position of the cantilever support. The same relationship of friction with velocity was also derived for the maximum spring force by Dudko et al. (2002). ΔF and v^* in equation (4) were derived as follows by Sang:

$$v^* = 2 \left(\frac{v \beta \omega_o^2 U_o}{k_B T \lambda} \right) \frac{\Omega_k^2}{(1 - \Omega_k^4)^{1/2}}; \quad (5a)$$

$$\Omega_k = \frac{\omega_o}{2\pi\omega_k}; \quad \omega_o = \sqrt{\frac{M\lambda^2}{U_o}}; \quad \omega_k = \sqrt{\frac{M}{k}}$$

$$\Delta F = \frac{\pi U_o}{\lambda} \left(\frac{3 k_B T}{2 U_o} \right)^{2/3} \left(\frac{(1 - \Omega_k^4)^{1/2}}{1 + \Omega_k^2} \right) \quad (5b)$$

In equations (5a and 5b) v is the velocity of the cantilever stage, β is the microscopic friction coefficient or dissipation (damping) factor, ω_o is the frequency of the small oscillations of the tip in the minima of the periodic potential, λ is the lattice constant, U_o is the surface barrier potential height, M and k represent the mass and the spring constant of the cantilever, respectively, and $2\pi\Omega_k$ represents the ratio of ω_o with the intrinsic cantilever resonance frequency ω_k .

Sang's and Dudko's model was experimentally confirmed by Sills and Overney (2003) on an unstructured amorphous surface of atactic polystyrene, Fig. 6.

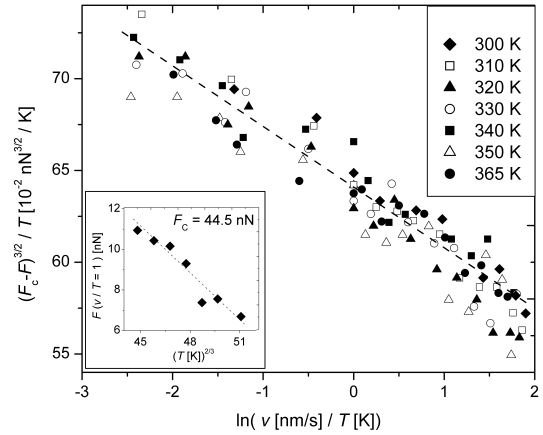


Figure 6. Collapse of SFM friction data obtained on atactic polystyrene using the ramped creep scaling model. The regression parameters from the linear fit (dashed line) are $-2.158 \times 10^{-2} \text{ N}^{3/2} \cdot \text{s/m}$ and $40.186 \times 10^{-2} \text{ nN}^{-3/2}/\text{K}$ ($R^2=0.9124$). Lower inset: the constant F_c is determined from the intercept of the friction force F versus $T^{2/3}$ for a fixed ratio $T/v = 1$ K/(nm/s): $F_c = 44.5$ nN. Adapted from Sills and Overney (2003)

Dudko pointed out that the typically used weak spring constants in SFM measurements are responsible for the more pronounced logarithmic behavior of friction in velocity as found by Gnecco et al. (2000) and He et al. (2002). The ramped creep model is also supported by numerical solutions of the Langevin equation.

The Langevin equation combines the equation of motion (including the sinusoidal

potential and perfect cantilever oscillator in the total potential energy E) with the thermal noise in the form of the random force, $\xi(t)$, i.e.,

$$M\ddot{x} + M\beta\dot{x} + \frac{\partial E(x,t)}{\partial x} = \xi(t) \quad (6)$$

$$\text{where } E(x,t) = \frac{k}{2}(R(t) - x)^2 - U_o \left(\frac{2\pi x}{\lambda} \right).$$

Equation (6) was solved numerically by both Sang et al. (2001) and Dudko et al. (2002) independently, assuming a Gaussian fluctuation-dissipation relation, $\langle \xi(t)\xi(t') \rangle = 2M\beta k_b T \delta t - t'$ to express the random force. Sang confirmed the *ramped creep model*, and Dudko showed that a force reconstruction approach from the density of states (accumulated from the corresponding Fokker-Planck equation) is equivalent to the Langevin equation. From the dynamic spectral analysis it could be concluded that the locked states (states within the potential wells) contribute mostly to the potential component of the friction force that dominates at low driving velocities, and sliding states contribute to viscous friction dominating at high driving velocities (Dudko et al. (2002)).

It should be noted that all of the above results considered an overdamped SFM system with respect to the driven spring (i.e., $\beta^2 > 4kM$), and an underdamped system with respect to the periodic potential (i.e., $\beta^2 < 4(M\omega)^2$). This aspect will be further addressed below in our discussion of metastable lubricant systems in large conforming contacts.

6. Limitation of the Gaussian Statistics – The Fractal Space

The spectral description of dynamic processes involving probability density functions has recently been the focus of numerous theoretical papers that treat various statistical kernels (Luedtke et al. (1999), Sokolov (2000), Metzler et al. (2000), Metzler et al. (2001)). Dudko et al. (2002)'s Fokker-Planck discussion of kinetic friction and Luedtke et al. (1999)'s Lévy flight model of slip diffusion of adsorbed nanoclusters are two examples in which statistical methods are applied to describe diffusive properties relevant to the kinetics in tribology.

Currently most models used to describe tribological processes assume Gaussian statistics

(e.g., Sang et al. (2001), and Dudko et al. (2002)). One of the limitations of a Gaussian statistics is that there are no correlations between statistical incidences. In other words, the Gaussian dynamic system is without memory. This is important to remember as the Eyring model discussed above, with its equally spaced potential barriers, used a Gaussian statistics. Simple "inert" lubricants, such as short chain alkanes embedded between silicon wafers, are described satisfactorily with such a statistics; however, confined complex liquids are not, such as branched molecules, polymers, and generally chemically interactive and entropically confined systems (e.g., perfluoropolyether lubricants as discussed below).

Confined complex liquids, for instance, easily exhibit strongly interacting glass-like behavior. The dynamic and stress relaxation behaviors in glasses, frequently discussed only including low interacting system with Arrhenius laws (Gaussian statistics), are often distorted from processes described by independently occurring microscopic processes. For instance, deviations from the Debye exponential relaxation as introduced in equation (1) are expressed in the form of an *extended exponential* Kohlrausch relaxation function over time t ; i.e.,

$$F(t) \equiv \left[\frac{X(t) - X(\infty)}{X(0) - X(\infty)} \right] = e^{-\left(\frac{t}{\tau}\right)^b}; \quad 0 < b < 1 \quad (7)$$

where X is the property that is relaxed. The exponent b , the Kohlrausch exponent, can theoretically be determined if one assumes that the process occurs in series, representing a well-determined microscopic origin that correlates the various degrees of freedom (Palmer et al. (1984)). This approach is borrowed from magnetic spin models such as the *Ising spin model* (Ashcroft et al. (1976)). The idea is that a given molecular motion is dependent on the availability of other degrees of freedom of mobile neighboring structural units. Finite relaxation times, t_{\max} , are gradually obtained with increasing spin levels (ergodic limit).

As mentioned above, the models by Dudko et al. (2002) and Sang et al. (2001) assumed Gaussian statistics. To illustrate how a diffusion process can deviate from Gaussian statistics, we

introduce a simplified version of the Langevin equation, i.e.,

$$\ddot{x} = -\eta\dot{x} + \zeta(t) \quad (8)$$

with the coordinate x , the dissipation (or dampening) parameter η , and the random acceleration $\zeta(t)$. Assuming Gaussian statistics, the mean squared displacement is

$$\langle x^2(t) \rangle = 2k_B T \eta t = 2Dt \quad (9)$$

where $D = \eta kT$ defines the diffusion constant (Becker (1985)). It was already realized at the time of Smoluchovski at the beginning of the 20th century that a diffusive description of a dynamic process demands a thermodynamically well-equilibrated or mixed system. Especially in a confined tribological system that involves a third medium (e.g., a lubricant), it can be expected that the Markovian nature of the underlying stochastic process could be disturbed. Consequently, for a monolayer lubricant that is chemically interacting, a nonlinear relationship of the mean squared displacement in time can be expected. Manifestations of anomalous transport are long-range spatial or temporal correlations. Two extreme limits can be distinguished: (a) processes with strong temporal relations ("fractal time") (Metzler et al. (2000)), and (b) systems that exhibit long jumps ("Lévy flights") (Metzler et al. (2001)).

7. Fractal Mobility in Reactive Lubrication

The importance of the underlying kinetics is illustrated by ultra-thin wetting lubricants. The spreading of "completely wetting" polymer liquids on solid surfaces has revealed unexpected spatial and temporal features when examined at the molecular level. The spreading profile is typically characterized by the appearance of a precursor film of monomolecular thickness extending over macroscopic distances and, in many cases, a terracing (also on the order of molecular dimensions) of the fluid remaining in the reservoir (Heslot et al. (1989)). These spatial features have been shown to be consistent with a Poiseuille-like flow in which the disjoining pressure gradients with film thickness drive the spreading process (Karis et al. (1999)). The

temporal evolution of the spreading profile in this film thickness regime is, however, found to universally scale as $t^{1/2}$ even at short times (Heslot et al. (1989)). That the spreading dynamics are reflective of a diffusive transport mechanism, and not of a pressure driven "liquid" flow, suggests that interfacial confinement substantially alters the mobility of molecularly thin polymer fluids (Burlatsky et al. (1996)).

The molecular mobility is of fundamental importance for monolayer lubrication purposes, such as in magnetic storage devices. It has, for instance, been shown that for low surface energy hydroxyl-terminated perfluoropolyether (PFPE-OH) films, the lubricant exhibits spatially terraced flow profiles indicative of film layering (Karis et al. (1999)) and spreading dynamics that are diffusive in nature (O'Connor et al. (1996), Ma et al. (1999)). In magnetic storage devices the hydroxylated chain ends of molecularly thin PFPE-OH films interact with the solid surface, an amorphous carbon surface, via the formation of hydrogen-bonds with the polar, carbon-oxygen functionalities located on the carbon surface. The bonding of the PFPE-OH polymer to carbon is predicated on the ability of the PFPE backbone to deliver spatially the hydroxyl end-group to within a sufficiently close distance to the surface active sites. Kinetic measurements probing the bonding of the PFPE-OH polymer to the carbon reveal two distinctive kinetic behaviors, as illustrated in Figure 7 at two representative temperatures: 50 °C and 90 °C for the two temperature regimes below 56 °C and above 85 °C. Below 56 °C the kinetics are described with a time-dependent (fractal time dependent) rate coefficient of the form

$$k(t) = k_0 t^{-1/2} \quad (10)$$

and at temperatures above 85 °C with the form

$$k(t) = k_0 t^{-1.0} \quad (11)$$

The initial bonding rate constants, k_0 , increased abruptly as the temperature rose above 50° C.

The bonding kinetics in the low-temperature regime is characteristic of a diffusion-limited reaction occurring from a glass-like state of the molecularly thin PFPE-OH film (Plonka et al. (1996)). The mobility of the PFPE chain in the glass-like state is limited by the propagation of holes or packets of free volume, which facilitate configurational rearrangements of the chain. The

onset of changes in the bonding kinetics at nominally $T > 56^\circ$ signifies a fundamental change in the mobility of the molecularly thin PFPE-OH film. Specifically, the transition in the fractal time dependence suggests that delivery of the hydroxyl moiety to the surface is no longer limited by hole diffusion, and the increase in the initial rate constant indicates an enhancement in the backbone flexibility. These results are consistent with a transition in the film from a glass-like to a liquid-like state in which the enhanced PFPE-OH segmental mobility results from rotations about the ether oxygen linkages in the chain that become increasingly facile. The time dependence observed in the high-temperature rate coefficients, $k(t) = k_B t^{-1.0}$ is characteristic of a process occurring from a confined liquid-like state in which the activation energy increases as the extent of the reaction increases.

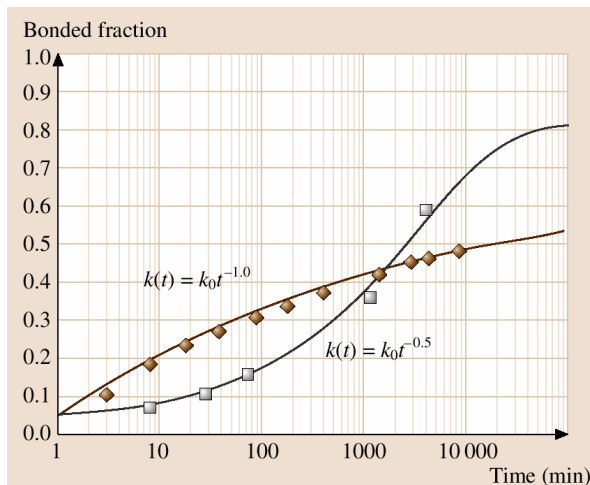


Figure 7. Representative kinetic data for the bonding of PFPE-OH (tradename: Fomblin Zdol) to amorphous carbon at $T = 50^\circ\text{C}$ and $T = 90^\circ\text{C}$. Solid lines represent fits using a rate coefficient of the form, $k(t) = k_0 t^{-\alpha}$ with $\alpha = 0.5$ for $T = 50^\circ\text{C}$ and $\alpha = 1.0$ for $T = 90^\circ\text{C}$.

The impact of this transition in the molecular mobility on tribology can be illustrated with sinusoidally modulated shear force experiments (Overney et al. (2000), (Ge et al. (2000))). In brief, a molecularly thin ($10.7 \pm 0.5 \text{ \AA}$) PFPE-OH film is subjected to a local shear stress by means of a sinusoidal force applied *laterally* to a SFM probe (at constant load) where the modulation amplitude is initially set below that required to initiate sliding between the tip and the sample. The amplitude

and phase-shift responses are measures of the contact stiffness and the effective viscous dampening, respectively. From Figure 8 it can be inferred that the SFM-measured nanorheological properties of the PFPE-OH film exhibit the changes discussed above in the molecular mobility. Thus kinetic and rheological data suggest that the thermal transition observed is due to the formation of a two-dimensional (2D) glass. The "glass transition" results from the preferential "freezing out" of the out-of-plane torsional motions of the energetically confined PFPE backbone. The confinement-induced solidification in the molecularly thin precursor film will significantly impact the lubrication properties and challenge thermodynamic, well-equilibrated models of lubrication as introduced above.

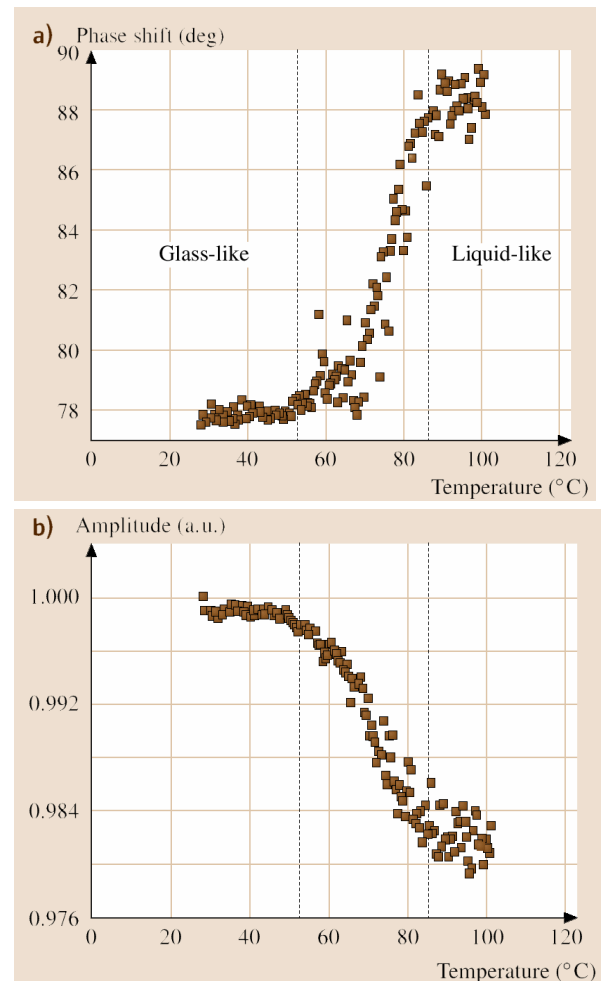


Figure 8. Shear-modulated SFM experiments performed on a $10.7 \pm 0.5 \text{ \AA}$ Fomblin Zdol film: a) phase shift response between disturbance and response, and b) contact stiffness response vs. temperature.

8. Metastable Lubricant Systems in Large Conforming Contacts

It is important to note that in an experiment of thermal activation, the critical time of the experiment t_{exp} decides the system response with its finite relaxation time t_{max} . If $t_{\text{exp}} > t_{\text{max}}$, the system behaves in an ergodic manner, and thermodynamic laws apply for interpreting lubrication results. On the contrary, if $t_{\text{exp}} < t_{\text{max}}$ the thermal evolution cannot be described by classical statistical thermodynamics. A metastable configuration is generated. The experimental time depends strongly on the contact area, the parameter that most differs between SFA and SFM measurements. SFA experiments involve large micron-scale contacts while SFM measurements are conducted with contacts on the nanoscale.

Because of the large contact area, SFA experiments are very susceptible to generating unequilibrated metastable lubricant configurations. The SFA study by Yoshizawa et al. (1993), in which distinctively different *dynamic states of friction* were introduced, could be interpreted as such. To date there are three velocity regimes used to describe the dynamic state of friction for a system that is "underdamped" (Rozman et al. (1996)). In an underdamped system, realized by a stiff spring compared to the friction constant, the characteristic slip time is comparable or smaller than the response time of the mechanical system. One distinguishes three velocity regimes, as depicted in Figure 9. The three regimes distinguish themselves by a single discriminator, v_c , a material, pressure and temperature dependent critical velocity. The regimes are described as

- (1) highly regular with high amplitude stick-slip for $v \ll v_c$,
- (2) intermittent stochastic stick-slip for $v < v_c$, and
- (3) smooth low friction sliding for $v > v_c$.

Various models have been suggested to describe the different dynamic states, including melting freezing transition (Carlson et al. (1996)), chain adsorption on substrates (Braiman et al. (1996)), and embedded particle (Rozman et al. (1996)). Until the embedded particle model

by Rozman was introduced, the SFA approach seemed to be the tool of choice to investigate metastable lubricant configurations. Rozman's single particle model alerts us however about drawing unambiguous conclusions on the dynamical structure of a molecular system embedded between two plates and driven by an underdamped system. In Rozman's simple theoretical model, sketched in Figure 10, a single particle is embedded between two corrugated surfaces (*two-wave potential*). The top plate is pulled at constant velocity by a linear spring and the plate motion is monitored. Interestingly, the plate exhibits exactly the same dynamic state of frictional motion as introduced above with the three regimes, which were attributed to a rate-dependent configurational change of the lubricant.

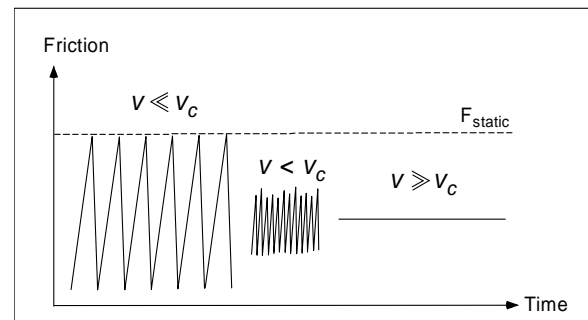


Figure 9. Dynamic states of friction for an underdamped spring system.

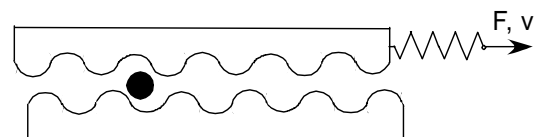


Figure 10. Model of single particle embedded in a two-wave potential driven at constant force, F , and velocity v .

Finally it shall be noted that the slip relaxation pattern depends on the condition under which the stick-slip motion is being studied. In an *overdamped* system, i.e., a system in which the spring constant is weak compared to the friction constant, Rozman et al. (1998b) found that one can control the experimentally observed relaxation pattern of the slip by controlling the spring constant.

9. Conclusion

Starting from a classical tribological Master Curve, the Stribeck curve, with its complex description of lubrication for thin lubricants, we launched a discussion of molecular lubrication pulling together disparate approaches to studying friction. We found that phenomenological descriptions of lubrication, such as the Reynold's theory, were kept alive for ultra-thin lubricants by "adjusting" material properties, such as the viscosity. This is a common engineering approach to introduce "effective" or "apparent" properties, if tested models fail to describe new situations.

In the case of molecular lubrication, significant progress has been made over the last ten years. Two instrumental techniques have in particular contributed to this progress: the SFA and the SFM. The contributions of these two techniques have been complementary. While the SFA has tested lubricants under pressure constraints with large contacts in respect to the size of the trapped molecules, the SFM has probed the degree of collective mobility with

disturbances in the size of the molecules themselves.

One feature common to interpreting lubrication results, and which was discussed here in detail, is the problem of finding the appropriate underlying statistics to describe the lubrication process. Most of the current molecular models that have been used to describe molecular friction and lubrication assumed a Gaussian statistics. Only recently has it been recognized important to consider statistics that embrace long-range spatial or temporal correlations. In the near future, it can be expected that the next leap in an improved fundamental understanding of kinetics and energetics in nanolubrication will come from interpretations that are challenging the Markovian nature of the underlying stochastic process.

References

- Ashcroft, N. W. and Mermin, N. D. (1976), *Solid State Physics*. CBS Publishing Asia Ltd., Philadelphia.
- Becker, R. (1985), *Theorie der Waerme*. Springer-Verlag, Berlin.
- Binnig, G., Quate, C. F. and Gerber, C. (1986), "Atomic Force Microscope", *Phys. Rev. Lett.* **56**, 930-933.
- Blunier, S., Zogg, H., Tiwari, A. N., Overney, R. M., Haefke, H., Buffat, P. and Kostorz, G. (1992), "Lattice and thermal misfit dislocations in epitaxial $\text{CaF}_2/\text{Si}(111)$ and $\text{BaF}_2/\text{CaF}_2/\text{Si}(111)$ structures", *Phys. Rev. Lett.* **68**, 3599-3602.
- Bowden, F. P. and Tabor, D. (1951), *The friction and lubrication of solids*. Clarendon Press, Oxford.
- Braiman, Y., Family, F. and Hentschel, H. G. E. (1996), "Array-enhanced friction in the periodic stick-slip motion of nonlinear oscillators", *Phys. Rev. E* **53**, R3005-8.
- Briscoe, B. J. and Evans, D. C. B. (1982), "The shear properties of Langmuir-Blodgett layers", *Proc. R. Lond. A* **380**, 389-407.
- Buenviaje, C., Ge, S., Rafailovich, M., Sokolov, J., Drake, J. M. and Overney, R. M. (1999), "Confined flow in polymer films at interfaces", *Langmuir* **19**, 6446-6450.
- Burlatsky, S. F., Oshanin, G., Cazabat, A. M. and Moreau, M. (1996), "Microscopic model of upward creep of an ultrathin wetting film", *Phys. Rev. Lett.* **76**, 86-9.
- Carlson, J. M. and Batista, A. A. (1996), "Constitutive relation for the friction between lubricated surfaces", *Phys. Rev. E* **53**, 4153-4164.
- Christenson, H. K., Gruen, D. W. R., Horn, R. G. and Israelachvili, J. N. (1987), "Structuring in Liquid Alkanes Between Solid-Surfaces - Force Measurements and Mean-Field Theory", *J. Chem. Phys.* **87**(3), 1834-1841.
- Dorinson, A. and Ludema, K. C. (1985), *Mechanics and Chemistry in Lubrication*. Elsevier, Amsterdam.
- Drummond, C. and Israelachvili, J. (2000), "Dynamic behavior of confined branched hydrocarbon lubricant fluids under shear", *Macromolecules* **33**(13), 4910-4920.
- Dudko, O. K., Filippov, A. E., Klafter, J. and Urbakh, M. (2002), "Dynamic Force Spectroscopy: A Fokker-Planck Approach", *Chem. Phys. Lett.* **352**, 499-504.
- Dudko, O. K., Filippov, A. E., Klafter, J. and Urbakh, M. (2002), "Dynamic force spectroscopy: a

- Fokker-Planck approach”, *Chemical Physics Letters* **352**, 499-504.
- Ge, S., Pu, Y., Zhang, W., Rafailovich, M., Sokolov, J., Buenviaje, C., Buckmaster, R. and Overney, R. M. (2000), “Shear modulation force microscopy study of near surface glass transition temperature”, *Physical Review Letters* **85**(11), 2340-2343.
- Glasstone, S., Laidler, K. J. and Eyring, H. (1941), *Theory of Rate Processes*. McGraw-Hill, New York.
- Gnecco, E., Bennewitz, R., Gyalog, T., Loppacher, C., Bammerlin, M., Meyer, E. and Güntherodt, H.-J. (2000), “Velocity Dependence of Atomic Friction”, *Phys. Rev. Lett.* **84**(6), 1172-1175.
- Hardy, W. B. and Doubleday, I. (1922), “Boundary Lubrication - The Paraffin Series”, *Proc. Roy. Soc. A* **100**, 550-574.
- He, M., Szuchmacher Blum, A., Overney, G. and Overney, R. M. (2002), “Effect of Interfacial Liquid Structuring on the Coherence Length in Nanolubrication”, *Phys. Rev. Lett.* **88**(15), 154302/1-4.
- Heslot, F., Fraysse, N. and Cazabat, A. M. (1989), “Molecular layering in the spreading of wetting liquid drops”, *Nature* **338**, 640-2.
- Heslot, F., Baumberger, T., Perrin, B., Caroli, B. and Caroli, C. (1994), “Creep, stick-slip, and dry-friction dynamics: experiments and a heuristic model”, *Phys. Rev. E* **49**, 4973-88.
- Israelachvili, J., P., McGuiggan G., M., Gee, M., Homola, A., Robbins, M. and Thompson, P. (1990), “Liquid Dynamics in Molecularly Thin Films”, *J. Phys.: Condens. Matter* **2**, 89-98.
- Johnson, K. L. (1987), *Contact mechanics*. Cambridge University Press, Cambridge; New York.
- Karis, T. E. and Tyndall, G. W. (1999), “Calculation of spreading profiles for molecularly-thin films from surface energy gradients”, *J. Non-Newtonian Fluid Mech.* **82**, 287-302.
- Luedtke, W. D. and Landman, U. (1999), “Slip Diffusion and Levy Flights of an Adsorbed Gold Nanocluster”, *Phys. Rev. Lett.* **82**, 3835-3838.
- Ma, X., Gui, J., Smoliar, L., Grannen, K., Marchon, B., Bauer, C. L. and Jhon, M. S. (1999), “Complex terraced spreading of perfluoropolyalkylether films on carbon surfaces”, *Phys. Rev. E* **59**, 722-7.
- Metzler, R. and Klafter, J. (2000), “The Random Walks Guide to Anomalous Diffusion: A Fractional Dynamics Approach”, *Phys. Reports* **339**, 1-77.
- Metzler, R. and Klafter, J. (2001), “Levy Meets Boltzmann: Strange initial Conditions for Brownian and Fractional Fokker-Planck Equations”, *Physica A* **302**, 290-296.
- Meyer, E., Overney, R. M., Dransfeld, K. and Gyalog, T. (1998), *Nanoscience: Friction and Rheology on the Nanometer Scale*. World Scientific, Singapore.
- O'Connor, T. M., Back, Y. R., Jhon, M. S., Min, B. G., Yoon, D. Y. and Karis, T. E. (1996), “Surface diffusion of thin perfluoropolyalkylether films”, *J. Appl. Phys.* **79**, 5788-90.
- Overney, R. M., Takano, H., Fujihira, M., Paulus, W. and Ringsdorf, H. (1994a), “Anisotropy in friction and molecular stick-slip motion”, *Phys. Rev. Lett.* **72**, 3546-49.
- Overney, R. M., Takano, H. and Fujihira, M. (1994b), “Elastic Compliances Measured by Atomic Force Microscopy”, *Europhys Lett* **26**(6), 443-447.
- Overney, R.M., Buenviaje, C., Luginbuehl, R. and Dinelli, F. (2000) “Glass and Structural Transitions measured at Polymer Surfaces on the Nanoscale”, *J. Thermal Analysis and Calorimetry*, **59**, 205-225.
- Palmer, R. G., Stein, D. L. and Abrahams, E. (1984), “Models of hierarchically constrained dynamics for glass relaxation”, *Phys. Rev. Lett.* **53**, 958-61.
- Plonka, A., Bednarek, J. and Pietrucha, K. (1996), “Reaction dynamics in glass transition region: propagating radicals in ultraviolet-irradiated poly(methyl methacrylate)”, *J. Chem. Phys.* **104**, 5279-83.
- Petrov, N. P. (1883), *Friction in Machines and the Effect of the Lubricant*, St. Petersburg.
- Reiter, G., Demirel, A. L., Peanasky, J., Cai, L. L. and Granick, S. (1994), “Stick to slip transition and adhesion of lubricated surfaces in moving contact”, *J. Chem. Phys.* **101**, 2606-15.
- Reynolds, O. (1886), “On the Theory of Lubrication and its Application to Mr. Beauchamp Tower's Experiments, Including an Experimental Determination of the Viscosity of Olive Oil”, *Phil. Trans. Roy. Soc.* **177**, 157-234.
- Rozman, M. G., Urbakh, M. and Klafter, J. (1996), “Stick-slip motion and force fluctuations in a driven two-wave potential”, *Phys. Rev. Lett.* **77**, 683-686.
- Rozman, M. G., Urbakh, M. and Klafter, J. (1998a), “Stick-slip dynamics of interfacial friction”, *Physica A* **249**, 184-189.
- Rozman, M. G., Urbakh, M. and Klafter, J. (1998b), “Controlling chaotic frictional forces”, *Phys. Rev. E* **57**, 7340-7343.
- Sang, Y., Dube, M. and Grant, M. (2001), “Thermal Effects on Atomic Friction”, *Phys. Rev. Lett.* **87**(17), 174301/1-4.
- Sills, S., and Overney, R. M. (2003), “Creeping friction dynamics and molecular dissipation

- mechanisms in glassy polymers", *Phys. Rev. Lett.* **91**(9), 095501(1-4), 2003.
- Sokolov, I. M. (2000), "Levy Flights From a Continuous-Time Process", *Phys. Rev. E* **63**, 011104/1-10.
- Tabor, D. and Winterton, R. H. S. (1969), "The direct measurement of normal and retarded van der Waals forces" , *Proc. R. Soc. Lond.* **A312**, 435-450.
- Tower, B. (1883), "First Report on Friction Experiments (Friction of Lubricated Bearings)", *Proc. Inst. Mech. Engrs* **Nov.**, 632-659.
- Yoshizawa, H., McGuiggan, P. and Israelachvili, J. N. (1993), "Identification of a second dynamic state during stick-slip motion", *Science* **259**, 1305-8.